

## Real-Time Studies of Iron Oxalate-Mediated Oxidation of Glycolaldehyde as a Model for Photochemical Aging of Aqueous Tropospheric Aerosols

### 3.1 Abstract

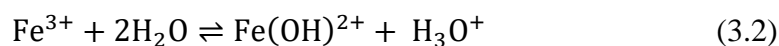
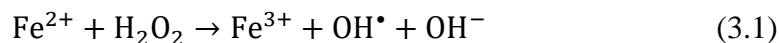
The complexation of iron (III) with oxalic acid in aqueous solution yields a strongly absorbing chromophore that undergoes photodissociation with high quantum yield to give iron (II) and the carbon dioxide anion radical. Importantly, this complex absorbs near-UV radiation ( $\lambda > 350$  nm), making it a potentially powerful source of oxidants in aqueous tropospheric chemistry. Although this photochemical system has been studied for several decades, the mechanistic details associated with its role in the oxidation of dissolved organic matter within cloud water, fog, and aqueous aerosol remain largely unknown. This study utilizes glycolaldehyde as a model organic species to study the oxidation pathways and evolution of organic aerosol initiated by the photodissociation of aqueous iron (III) oxalate complexes. Hanging droplets (radius 1 mm) containing iron (III), oxalic acid, glycolaldehyde, and ammonium sulfate (pH ~ 3) are exposed to irradiation at 365 nm and sampled at discrete time points utilizing field-induced droplet ionization mass spectrometry (FIDI-MS). Glycolaldehyde is found to undergo rapid oxidation to form glyoxal, glycolic acid, and glyoxylic acid, but the formation of high-molecular-weight oligomers is not observed. These results suggest that photodissociation of iron (III) oxalate can lead to the formation of volatile oxidation products in tropospheric aqueous aerosol.

## 3.2 Introduction

Tropospheric aqueous-phase chemistry plays a key role in the aging of dissolved organics in the atmosphere.<sup>4-6,124,125</sup> Aqueous phase processing may occur as a result of “dark” reactions such as acid catalysis, hydration, and oligomerization,<sup>126,127</sup> or they may result from photochemical excitation of dissolved light-absorbing species.<sup>128-130</sup> One of the key components directing the aging of dissolved organics is the availability of oxidative species such as the hydroxyl radical (OH) and hydrogen peroxide (H<sub>2</sub>O<sub>2</sub>), which may be present by direct generation in solution or by uptake from the gas phase.<sup>131</sup> Many laboratory studies have investigated SOA production initiated by photolysis of dissolved H<sub>2</sub>O<sub>2</sub>.<sup>132-135</sup> There is increasing evidence, however, that processes involving the photolysis of photoactive organic and organometallic compounds may also be important sources of highly reactive aqueous oxidants.<sup>129,136-138</sup>

Transition metal ions present in cloudwater or aqueous aerosol are known to undergo photo-initiated electron transfer processes that can be a significant source of oxidative species.<sup>6,90,139</sup> Iron, the most abundant transition metal ion in tropospheric particles, can be found in aerosol originating from sea spray,<sup>140</sup> mineral dust,<sup>90</sup> and anthropogenic emissions.<sup>93</sup> Measured concentrations of iron in fog waters range from micromolar or less in rural areas to tens of micromolar in highly polluted environments.<sup>141</sup> As a result of these substantial concentrations, iron can play an important role in the aqueous-phase tropospheric oxidation of organics. The reactions of dissolved iron-hydroxy complexes, or the Fenton reactions, are a well-characterized source of atmospheric oxidants.<sup>91,92,142</sup> The direct reaction of hydrogen peroxide with iron (II) yields hydroxyl radicals in the dark

Fenton reaction (3.1), whereas the photo-Fenton reaction yields hydroxyl radicals by photolysis of the iron (III) hydroxy complex (3.2 and 3.3).

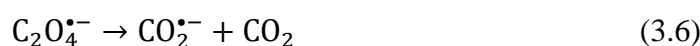
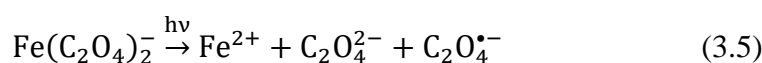
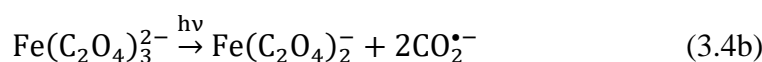
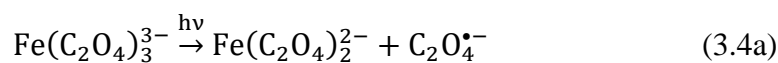


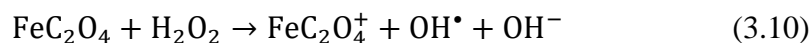
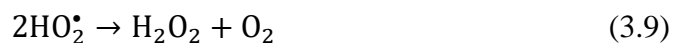
Several groups have recently explored the impact of iron photochemistry on SOA formation. Chu and co-workers studied the effects of iron (II) sulfate and iron (III) sulfate seed aerosol on SOA formation at 50% RH and found that iron (II) complexes inhibited SOA formation, whereas iron (III) had little effect on SOA formation.<sup>143</sup> They attributed the effect of iron (II) to the reduction of organic condensate by the iron species and subsequent disruption of oligomerization processes. Nguyen and co-workers investigated the uptake and oxidation of glycolaldehyde in aqueous aerosol containing hydrogen peroxide and iron complexes.<sup>91</sup> They found that the photo-Fenton reaction significantly increased the degree of oxidation in aerosol particles when compared with H<sub>2</sub>O<sub>2</sub> photolysis alone (ratio of O/C=0.9 with iron and H<sub>2</sub>O<sub>2</sub> vs. O/C=0.5 with H<sub>2</sub>O<sub>2</sub>).

Although laboratory experiments have demonstrated that photo-Fenton chemistry can lead to significant oxidation of organics,<sup>144-146</sup> the role of such processes in ambient aerosol is not clear, as the reactions are highly dependent on pH, iron concentration, and the concentration of other ligands that readily complex with iron.<sup>92,147,148</sup> Notably, the formation of stable complexes between iron and dicarboxylate ligands can have a significant impact on the photochemical reaction pathways. Complexation between the oxalate anion, one of the most abundant low-molecular weight organic compounds found

in aqueous aerosol,<sup>93,149-151</sup> and iron has long been known to generate significant yields of oxidative species by photochemical reduction of iron. Initially studied as a chemical actinometer,<sup>152,153</sup> seminal work by Zuo and Hoigné demonstrated that photolysis of iron oxalate complexes could lead to the generation of oxidative species under atmospherically relevant conditions.<sup>92</sup>

The proposed pathway for the photochemical generation of oxidative species from iron (III) oxalate complexes is shown in reactions 3.4-3.10 below. Depending on the pH, ionic strength, and concentration of iron and oxalate, three complexes are formed:  $\text{Fe}(\text{C}_2\text{O}_4)^+$ , which has low photochemical reactivity,<sup>154</sup> and  $\text{Fe}(\text{C}_2\text{O}_4)_2^-$  and  $\text{Fe}(\text{C}_2\text{O}_4)_3^{3-}$ , both of which undergo photochemical reduction of iron with high quantum yield.<sup>147,155</sup> The mechanism of photochemical dissociation of  $\text{Fe}(\text{C}_2\text{O}_4)_3^{3-}$  has been investigated in detail, with two groups presenting evidence for either intermolecular electron transfer (3.4a) or intramolecular electron transfer (3.4b) as the primary reaction pathway.<sup>156-159</sup> The mechanism of dissociation of  $\text{Fe}(\text{C}_2\text{O}_4)_2^-$  has not been studied extensively but is also expected to yield the oxalate anion radical, which rapidly dissociates to  $\text{CO}_2$  and  $\text{CO}_2^{\bullet-}$  (reactions 3.5 and 3.6).<sup>92</sup> The subsequent reaction of  $\text{CO}_2^{\bullet-}$  with  $\text{O}_2$  leads to the eventual formation of  $\text{H}_2\text{O}_2$  (reactions 3.7-3.9), which can then interact directly with  $\text{Fe}^{2+}$  (reaction 1) or with  $\text{FeC}_2\text{O}_4$  (reaction 3.10) to produce  $\text{OH}$ .<sup>160</sup>





Although the mechanism and kinetics of dissociation of iron (III) oxalate complexes have been examined in detail, much less information is available on the oxidation of atmospherically relevant compounds by this photochemical system. Zuo and Zhan found that the presence of iron (III) oxalate complexes increases the rate of oxidation of sulfur dioxide compared to iron alone under atmospherically relevant conditions.<sup>161</sup> In field sampling studies, Sorooshian et al. found an inverse correlation between concentrations of dissolved iron and oxalate in stratocumulus cloudwater above the northeastern Pacific ocean, suggesting that ferrioxalate photochemistry may play an important role in determining cloudwater composition under certain conditions.<sup>93</sup> These studies serve as initial demonstrations of the potential importance of such reactions in aqueous tropospheric chemistry, but further laboratory and field studies are necessary to better discern the complex interplay of reactions influencing the oxidation of dissolved organic compounds.

Glycolaldehyde serves as an excellent model system to study the influence of liquid-phase ferrioxalate photochemistry on the oxidation of dissolved organics. A major product of isoprene oxidation, glycolaldehyde is produced with an estimated global flux of greater than 42 Tg C yr<sup>-1</sup>.<sup>133,162,163</sup> The abundance of glycolaldehyde, along with its high solubility,<sup>164</sup> means that its oxidation processes may play a significant role in the formation of SOA in aqueous aerosol.

This study explores the photochemically initiated reaction pathways involved in the oxidation of aqueous glycolaldehyde in the presence of ferrioxalate complexes. Real-time studies of photochemical reactions in microliter droplets utilizing field-induced droplet ionization mass spectrometry (FIDI-MS)<sup>83,84</sup> provide insight into the changes in chemical composition of this model system upon UV irradiation.

### **3.3 Materials and Methods**

#### **3.3.1 Materials**

High-purity water and ACS-grade sulfuric acid were obtained from EMD Millipore (Billerica, MA). Concentrated ammonium hydroxide (28-30% by weight) and ACS-grade iron (iii) chloride 6-hydrate were obtained from J.T. Baker Avantor (Center Valley, PA). All other chemicals were purchased from Sigma-Aldrich (St. Louis, MO). Stock solutions were prepared in concentrations of 10-100 mM and stored at  $-20^{\circ}$  C with the exception of iron (iii) chloride stock solutions, which were prepared fresh daily at a concentration of 50 mM in a 5 mM solution of  $H_2SO_4$ .

#### **3.3.2 Field-Induced Droplet Ionization Mass Spectrometry**

The FIDI-MS source employed in this study is based upon an initial design described by Grimm and co-workers.<sup>83</sup> The general design and features of the updated source are described here, with further details given in Appendix A. A hanging droplet of 1.5-2 mm in diameter (2-4  $\mu$ L) is suspended on the end of a stainless steel capillary between two parallel plate electrodes separated by 6.3 mm (Figure 3.1c). The parallel plates are mounted to a translation stage to allow alignment of an aperture in the electrically grounded plate with the atmospheric pressure inlet of an LTQ-XL mass spectrometer (Thermo-Fisher,

Waltham, MA). The capillary is mounted on a separate translation stage to provide for placement of the droplet midway between the two plates in alignment with the inlet of the LTQ-XL. A droplet is formed from liquid fed through the capillary using a computer-controlled motorized syringe pump. Mass spectrometric sampling of the hanging droplet is accomplished by application of a pulsed high voltage (typically 3-5 kV, 100 ms duration) to the back parallel plate and to the suspended capillary at half the magnitude applied to the back plate to maintain field homogeneity between the front and back plate. When a sufficiently high voltage is applied, the electrical forces overcome the surface tension of the droplet, resulting in the bipolar ejection of highly-charged progeny droplets of less than 1  $\mu\text{m}$  in diameter from the opposite ends of the suspended droplet.<sup>84,85</sup> Charged droplets of a specific polarity enter the transfer capillary of the mass spectrometer, resulting in the detection of gas-phase ions in a manner similar to electrospray ionization.<sup>111</sup> Sampling of either positive or negative ions is achieved by switching the polarity of the high voltage applied to the back plate and capillary. The pulsed high voltage is controlled by a custom power supply and LabView software described elsewhere.<sup>165</sup>

The entire FIDI source is mounted within a custom enclosure that provides control of the environment in which the droplet is suspended, as shown in Figure 3.1a,b. The enclosure is equipped with a fused silica window to allow for the study of photochemical reactions and for visual droplet monitoring during experiments. To study the photochemistry of suspended droplets in the absence of oxygen, the chamber was flushed with nitrogen at a flow rate of 1.2 L/min for ~10 minutes prior to sampling, and the flow of nitrogen was maintained throughout the experiment; the sample was also degassed by bubbling with nitrogen. For all other experiments undertaken in this work, the enclosure was left open to

laboratory air. Photochemical reactions in the hanging droplet are accomplished by irradiation with 365 nm light with a radiant flux of approximately 5 mW generated by a fiber optic-coupled LED (FCS-0365-000, Mightex Systems, Pleasanton, CA). The light is focused onto the droplet using a collimating lens (74-UV, Ocean Optics, Dunedin, FL) and a spherical focusing lens. Based upon the estimated focal spot size (3 mm radius), the droplet size (1 mm radius), and the estimated radiant flux based on manufacturer ratings, the photon flux encountering the hanging droplet is estimated to be  $3 \times 10^{16}$  photons  $\text{cm}^{-2}$   $\text{s}^{-1}$ , approximately two orders of magnitude greater than the solar actinic flux at 365 nm with a 30° solar zenith angle.<sup>166</sup>

Photochemical experiments employing FIDI-MS were performed in solutions containing 0.5 mM  $\text{H}_2\text{SO}_4$ , 100  $\mu\text{M}$   $\text{NH}_3$ , 50  $\mu\text{M}$   $\text{FeCl}_3$ , 250  $\mu\text{M}$  oxalic acid, and 250  $\mu\text{M}$  glycolaldehyde. Control experiments were also performed by excluding iron, oxalic acid, or glycolaldehyde from the mixture and observing the impact on the photochemistry. In a typical experiment, a droplet of the solution was formed on the end of the capillary and allowed to rest for 1 minute prior to exposure to 365 nm radiation. Individual droplets were then sampled by application of a high voltage pulse after 0, 1, 2, and 3 min of irradiation. The presented spectra are averaged from four experiments on discrete droplets at each time point. Between experiments, the sample line was rinsed thoroughly with 10 mM  $\text{H}_2\text{SO}_4$  and was also allowed to soak overnight in this solution to prevent the accumulation of iron precipitates.



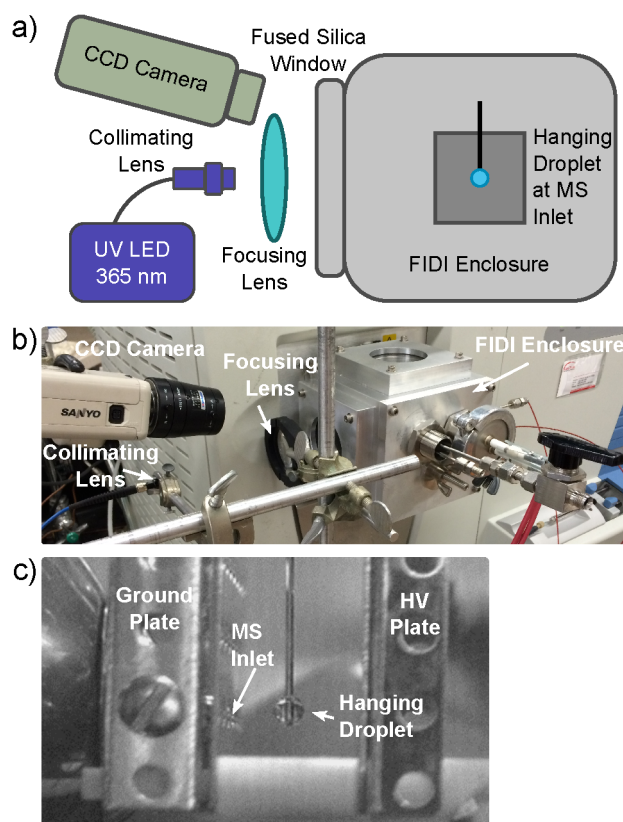


**Figure 3.1.** Experimental apparatus for studying photochemistry utilizing FIDI-MS. The primary components of the system are depicted schematically in (a) and shown as utilized in the laboratory in (b). A CCD camera image of the FIDI region is shown in (c).

## 3.4 Results and Discussion

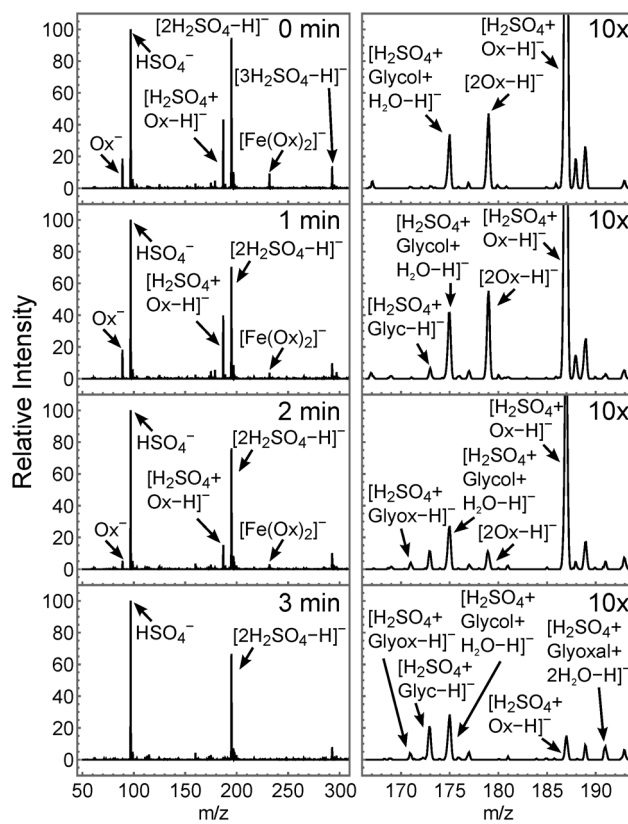
### 3.4.1 Oxidation of Glycolaldehyde by Iron (III) Oxalate Photochemistry

Figure 3.2 shows the FIDI-MS spectra of hanging droplets containing iron (III) oxalate complexes and glycolaldehyde exposed to irradiation at 365 nm for 0-3 minutes. The  $\text{HSO}_4^-$  anion and its dimer are the most prominent ions in the spectrum due to the high concentration of sulfate in solution (0.5 mM) utilized to achieve a pH of  $\sim 3$ . Oxalic acid (Ox) is also detected prior to irradiation (0 min) as a monomer, homodimer, and heterodimer with hydrogen sulfate ( $m/z$  89, 179, and 187, respectively), and the dimer of

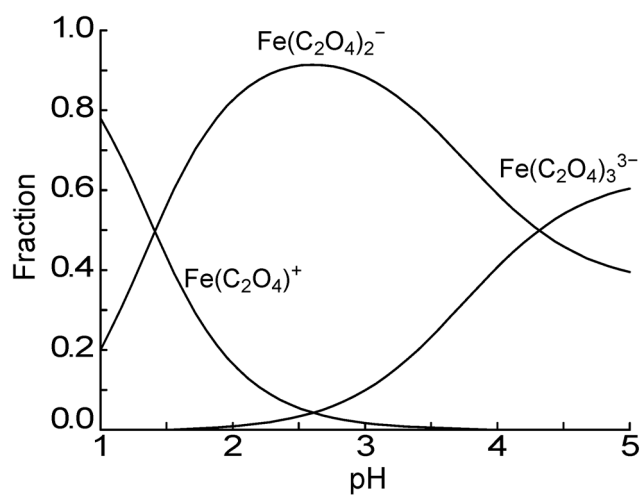
glycolaldehyde hydrate (Glycol+H<sub>2</sub>O) with hydrogen sulfate is also observed at m/z 175.

The Fe(C<sub>2</sub>O<sub>4</sub>)<sub>2</sub><sup>-</sup> ion, predicted by equilibrium calculations to be the dominant complex of iron (III) in the sample (Figure 3.3), is detected at m/z 232.

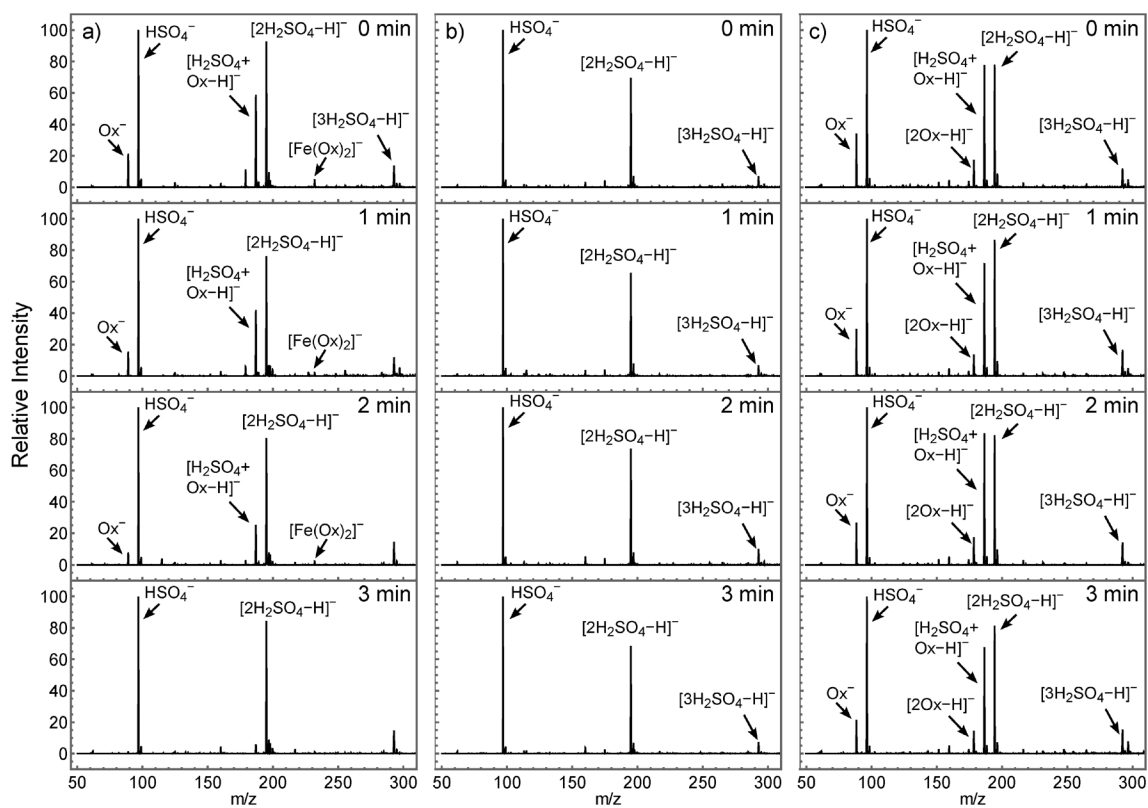
Upon irradiation, the Fe(C<sub>2</sub>O<sub>4</sub>)<sub>2</sub><sup>-</sup> complex and oxalic acid ions are rapidly depleted, and new ions are observed at m/z 173, 175, and 191. These photochemical oxidation products are assigned to glycolic acid (Glyc, m/z 173), glyoxylic acid (Glyox, m/z 171), and glyoxal hydrate (m/z 191), all observed as adducts with hydrogen sulfate. Formic acid is also observed as a dimer with hydrogen sulfate at m/z 143 with low intensity after 3 min of irradiation. It is possible that these ions represent the formation of organosulfate compounds rather than noncovalent complexes, but the free glycolic acid and glyoxylic acid ions (m/z 73 and 75, respectively) also increase in intensity over the course of the experiment, suggesting that the observed species are likely adducts formed during gas-phase ion generation.<sup>134</sup> The formation of these product ions is not observed in control experiments in which iron, glycolaldehyde, or oxalic acid is excluded from the reaction mixture (Figures 3.4 and 3.5).



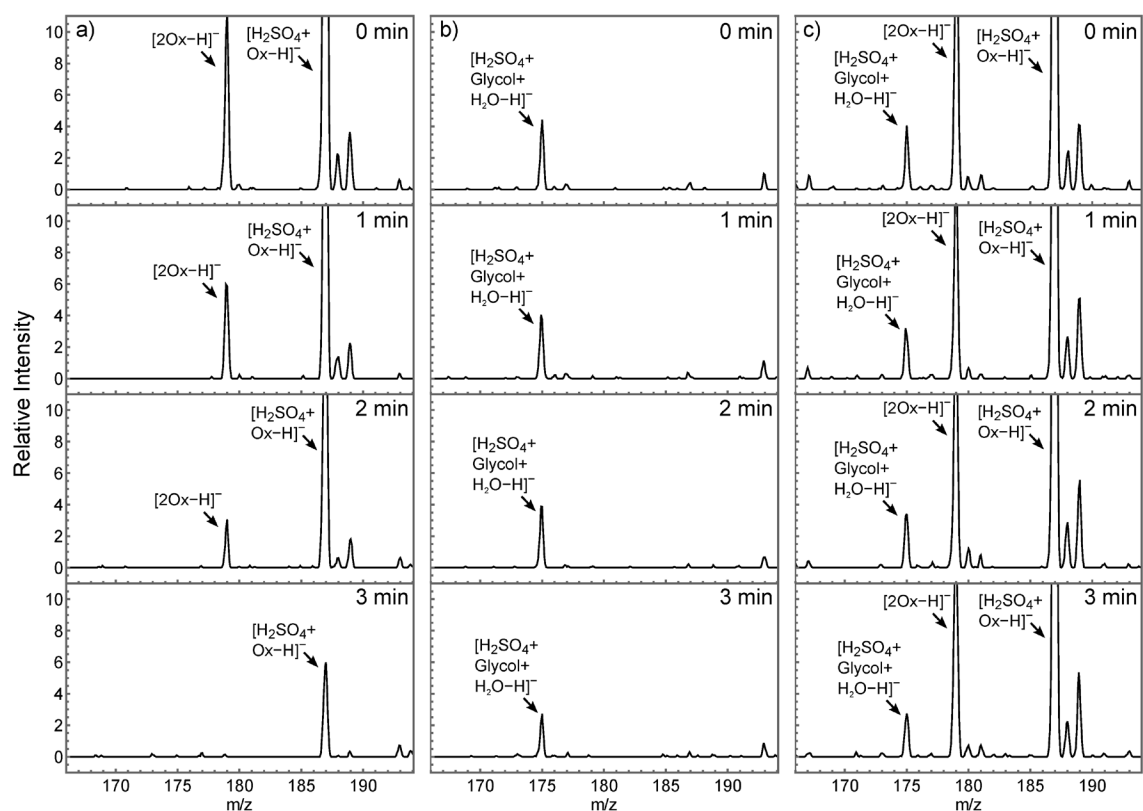
**Figure 3.2.** Monitoring the photochemistry of aqueous glycolaldehyde and iron (III) oxalate complexes by FIDI-MS. The left column shows the full spectrum, and the right column highlights the region where glycolaldehyde and its oxidation products are detected (10x zoom). The depletion of  $\text{Fe}(\text{C}_2\text{O}_4)_2^-$  and oxalic acid ( $\text{Ox}$ ) are clearly observed over the course of three minutes, and the oxidation of glycolaldehyde (glycol) to glycolic acid (glyc), glyoxylic acid (glyox), and glyoxal is observed.



**Figure 3.3.** Speciation of soluble iron (III) as a function of pH under conditions utilized for FIDI-MS experiments. Solution conditions:  $[\text{Fe}^{3+}] = 50 \mu\text{M}$ ,  $[\text{Cl}^-] = 150 \mu\text{M}$ ,  $[\text{H}_2\text{C}_2\text{O}_4] = 250 \mu\text{M}$ ,  $[\text{H}_2\text{SO}_4] = 0.5 \text{ mM}$ ,  $[\text{NH}_3] = 100 \mu\text{M}$ . Fractions were calculated using the MEDUSA program (*MEDUSA-Make Equilibrium Diagrams Using Sophisticated Algorithms*, Puigdomenech, I. Royal Institute of Technology 100 44 Stockholm, Sweden; 2010).

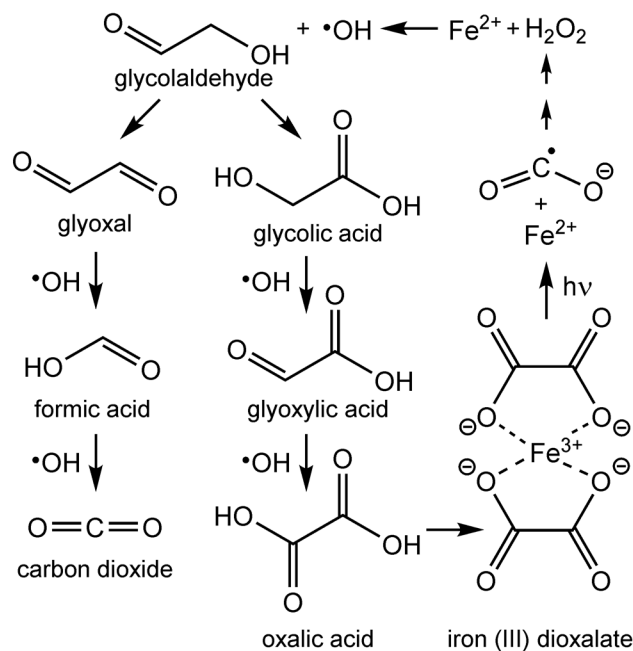


**Figure 3.4.** Control experiments for the oxidation of glycolaldehyde by photodissociation of iron (III) oxalate complexes; (a) iron (III) and oxalic acid only (no glycolaldehyde added), (b) iron (III) and glycolaldehyde only (no oxalic acid added), (c) glycolaldehyde and oxalic acid only (no iron added).



**Figure 3.5.** Control experiments for the oxidation of glycolaldehyde by photodissociation of iron (III) oxalate complexes, zoom on product region; (a) iron (III) and oxalic acid only (no glycolaldehyde added), (b) iron (III) and glycolaldehyde only (no oxalic acid added), (c) glycolaldehyde and oxalic acid only (no iron added).

The observed chemistry of the glycolaldehyde-ferrioxalate systems is summarized in Scheme 3.1. As described in reactions 3.4-3.10, photodissociation of iron oxalate complexes leads to the formation of hydroxyl radicals that oxidize glycolaldehyde to form glyoxal and glycolic acid. Further oxidation yields formic acid and glyoxylic acid from glycolaldehyde and glycolic acid, respectively. Glyoxylic acid may then undergo one final oxidation process to regenerate oxalic acid, whereas formic acid oxidation leads to the formation of carbon dioxide. The observed oxidation pathways are similar to those observed by Perri and co-workers for the oxidation of aqueous glycolaldehyde by hydroxyl radicals produced by H<sub>2</sub>O<sub>2</sub> photolysis initiated by a 254 nm Hg lamp.<sup>133</sup> Perri and co-workers also detected higher molecular weight oligomers in significant abundance and identified malonic and succinic acid as two of the major oligomerization products. Further study by Ortiz-Montalvo and co-workers identified malic and tartaric acids as additional oligomerization products.<sup>167</sup> Similarly, in a study of aerosol formation from reactive uptake of glycolaldehyde on seed aerosol doped with iron and H<sub>2</sub>O<sub>2</sub>, Nguyen and co-workers proposed that oligomerization products of glycolaldehyde contributed to the high observed O/C ratios of aerosol organics. In contrast, the FIDI-MS experiments presented in this study did not detect the formation of any oligomers in significant abundance. The comparatively high flux of oxidative species produced by the photodissociation of iron (III) oxalate complexes may favor sequential oxidation over oligomerization under the conditions utilized in this study.

**Scheme 3.1.** Oxidation Pathway of Glycolaldehyde in the Presence of Iron (III) Oxalate Complexes

### 3.4.2 Iron Oxalate Photochemistry Under Deoxygenated Conditions

The photochemistry of the iron (III) oxalate and glycolaldehyde system was also investigated in the absence of oxygen by purging both the sample solution and the reaction chamber with nitrogen gas. As shown in Figure 3.6, little change in the composition of the droplets is observed during irradiation under such conditions. In contrast to the nearly complete depletion of oxalate in the presence of oxygen, the ions associated with oxalic acid are only marginally reduced in intensity over the course of the reaction. In addition, the intensity of the  $\text{Fe}(\text{C}_2\text{O}_4)_2^-$  ion is significantly diminished after 1 min of irradiation, and minimal signal from oxidation products of glycolaldehyde is observed.



The absence of glycolaldehyde oxidation products in deoxygenated solutions is readily explained by the necessity of oxygen for the generation of hydroxyl radicals as detailed in reactions 3.4-3.10. The small amount of oxidation observed is attributed to trace concentrations of oxygen gas in the reaction chamber. The presence of oxygen is also necessary for the regeneration of iron (III) following photo-initiated reduction. Weller and co-workers recently measured a quantum yield of  $0.8 \pm 0.1$  for iron (II) formation under conditions similar to those utilized in this study, indicating that iron (III) should be rapidly depleted in the absence of oxygen.<sup>147</sup> Consistent with this result, we do not observe the  $\text{Fe}(\text{C}_2\text{O}_4)_2^-$  ion following irradiation in a nitrogen atmosphere. Similarly, little change in the intensity of oxalate ions is observed, as only 20-30% of the oxalic acid can be dissociated before all of the iron present is reduced. Zuo and Hoigné also observed that nearly all of the iron (III) was reduced to iron (II) rapidly in deoxygenated solutions, whereas in oxygenated solutions a steady state was reached once approximately 70% of the iron (III) was reduced.<sup>92</sup>

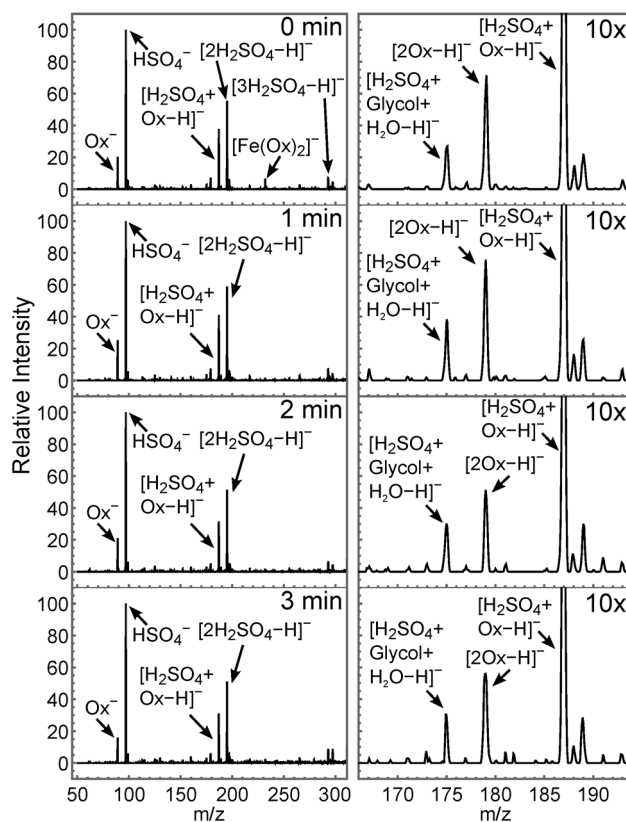


**Figure 3.6.** Photochemistry of deoxygenated solutions of iron (III) oxalate and glycolaldehyde. The full spectrum is shown on the left, and the right column shows a 10x zoom on the region of detection for glycolaldehyde and its oxidation products. In the absence of dissolved oxygen, little oxidation of glycolaldehyde is observed, and oxalate is not depleted over the course of the experiment. The  $\text{Fe}(\text{C}_2\text{O}_4)_2^-$  ion is substantially depleted after 1 min of irradiation.

### 3.5 Conclusions

The photochemical dissociation of iron (III) oxalate complexes has been studied for over a half-century, yet new research into this chemical system continues to yield insight into both the fundamental mechanism of dissociation and its coupling to complex chemical systems. In the context of aqueous tropospheric chemistry, there is still a great deal of uncertainty as to the role this species might play in the aging of aqueous SOA. This study presents initial investigations into the oxidation of dissolved organics by photodissociation of complexes of iron (III) oxalate using glycolaldehyde as a model compound. Studies of photolysis in suspended microliter droplets by FIDI-MS show that glycolaldehyde is readily oxidized to glycolic acid, glyoxylic acid, and glyoxal upon 365 nm photodissociation of iron oxalate complexes. These results are in good agreement with previous studies of aqueous glycolaldehyde oxidation by Turpin and co-workers.<sup>133,134,167</sup> The formation of oligomers in significant abundance is not observed, which is attributed to the rapid oxidation of organic species, leading to the generation of CO<sub>2</sub> or regeneration of oxalic acid. These results suggest that, under the appropriate conditions, the presence of iron and oxalate in aqueous tropospheric aerosol can lead to significant oxidation of dissolved organic material. Because of the high flux of near-UV photons in the troposphere, these reactions are expected to lead to the rapid generation of oxidizing species and the depletion of oxalic acid in the presence of iron, in agreement with recent field studies.<sup>93</sup> Further laboratory investigations into the role of iron (III) oxalate photochemistry in reactive uptake, along with additional field measurements, are necessary to better constrain the role of such complexes in aqueous tropospheric photochemistry.